In vitro anti-angiogenic effects of *Hemidesmus indicus* in hypoxic and normoxic conditions

L. Ferruzzi[a§], E. Turrini[a§], R. Gotti [b], A. Guerrini[c], M. Tacchini[c], G. Teti[d], M. Falconi[d], P. Hrelia[b], C. Fimognari[a*]

[a] Department for Life Quality Studies, Alma Mater Studiorum-University of Bologna, 47921 Rimini, Italy

[b] Department of Pharmacy and BioTechnology, Alma Mater Studiorum-University of Bologna, 40126 Bologna, Italy

[c] Department of Life Sciences and Biotechnologies, University of Ferrara, 44121 Ferrara, Italy

[d] Department of Biomedical and Neuromotor Sciences, Alma Mater Studiorum-University of Bologna, 40126 Bologna, Italy

§: Both authors contributed equally to this work.

*Corresponding author. Tel.: +39 051 2095636; fax: +39 051 2095624.

E-mail address: carmela.fimognari@unibo.it

Abstract

Ethnopharmacological relevance: The decoction of the roots of *Hemidesmus indicus* is widely used in the Indian traditional medicine for many purposes and poly-herbal preparations containing Hemidesmus are often used by traditional medical practitioners for the treatment of cancer. In the context of anticancer pharmacology, anti-angiogenic therapy has become an effective strategy for inhibiting new vessel formation and contrast tumor growth. These considerations are supported by the evidence that most tumors originate in hypoxic conditions and limitation of oxygen diffusion stimulates the formation of tumor abnormal microvasculature. Aim of this study was to evaluate the *in vitro* anti-angiogenic potential of *Hemidesmus indicus* (0.31–0.93mg/mL) on human umbilical vein endothelial cells and delineate the main molecular mechanisms involved in its anti-angiogenic activity both innormoxia and hypoxia.

Materials and methods: The decoction of *Hemidesmus indicus* was subjected to an extensive HPLC phytochemical characterization. Its *in vitro* anti-angiogenic potential was investigated in normoxia and hypoxia. Cell proliferation, apoptosis induction, and inhibition of endothelial cell migration and invasion were analyzed by flow cytometry. The endothelial tube formation assay was evaluated in matrixgel. The capillary tube branch points formed were counted using a MoticAE21 microscope and a VisiCam videocamera. The regulation of key factors of the neovascularization process such as VEGF, HIF-1α and VEGFR-2 was explored at mRNA and protein level by realtime PCR and flowcytometry, respectively.

Results: Treatment with Hemidesmus resulted in a significant inhibition of cell proliferation and tube formation in both normoxia and hypoxia. Hemidesmus differently regulated multiple molecular targets related to angiogenes is according to oxygen availability. In normoxia, the inhibition of VEGF was the main responsible for its anti-angiogenic effect; the angiogenes is inhibition induced in hypoxia was regulated by a more complex mechanism involving firstly HIF-1α inhibition, and then VEGF and VEGFR-2down-regulation. Additionally, the inhibition of endothelial cell migration and invasion by Hemidesmus was more pronounced in normoxia than in hypoxia, possibly due to the physiological enhanced induction of invasion characteristic of hypoxia.

Conclusions: Our results indicate that Hemidesmus might represent a promising therapeutic strategy for diseases in which the inhibition of angiogenesis could be beneficial, such as cancer. The antiangiogenic activity of Hemidesmus is based on multiple interactions with critical steps in the angiogenic cascade. VEGF expression stimulated by HIF-1α as well as endothelial cell migration and differentiation represent important targets of Hemidesmus action and might contribute to its cancer therapeutic efficacy that is presently emerging and offer a scientific basis for its use in traditional medicine.

Keywords: *Hemidesmus indicus*, HIF-1α, VEGF, anti-angiogenesis, anti-metastasis

Abbreviations:

7-AAD, 7-amino-actinomycin D; DMSO, dimethylsulfoxide; EHS, Engelbreth Holm-Swarm; FBS, fetal bovine serum; HI, *Hemidesmus indicus*; HIF-1α, hypoxia inducible factor-1α; HUVECs, human umbilical vein endothelial cells; VEGF, vascular endothelial growth factor; VEGFR, VEGF receptors; PE, phycoerythrin.

Introduction

Angiogenesis covers a key role in the development and spread of tumor. Cancer cells are not able to grow in diameter more than 1-2 mm^3 and metastasize without blood circulation. Tumor cells need blood vessels that bring oxygen and nutrients and remove metabolic wastes to spread. In absence of vascular support, tumors may become necrotic or even apoptotic (Parangi et al., 1996). Most tumors originate in hypoxic conditions and limitation of oxygen diffusion stimulates the formation of tumor abnormal microvasculature (Jain, 2005). The hypoxic condition enhances the transcription of vascular endothelial growth factor (VEGF) by hypoxia inducible factor-1α (HIF-1α) (Kuschel et al., 2012). An improved activity of VEGF has been reported in most aggressive cancers and it is related with a poor prognosis (Foekens et al., 2001).

The pivotal role of angiogenesis in tumor spread and metastasis formation provides the rationale for using anti-angiogenic strategies as a form of anticancer treatment. Thus, the inhibition of VEGF-signaling pathway is an interesting therapeutic strategy in the treatment of cancer and the most validated anti-angiogenic strategy targets the VEGF axis. Bevacizumab, the first clinically available angiogenesis inhibitor, directly blocks VEGF, and other drugs such as sunitinib, sorafenib and pazopanib indirectly inhibit VEGF receptor (VEGFR) activity (Cesca et al., 2013). Several angiogenesis inhibitors have been approved by FDA for cancer treatment, but their use is associated with many side effects, among them bleeding is one of the most severe (Elice and Rodeghiero, 2012).

Hemidesmus indicus (L.) R.Br. (HI) belongs to the family of *Asclepiadaceae* and is an Indian weed widely used in the traditional medicine. The plant is a bush, woody, with thick and brown bark, which grows from the upper Gangetic plains East-wards to Assam, throughout Central, Western and Southern India. Several *in vitro* and *in vivo* studies reported its anticancer, antioxidant, anti-inflammatory, antipyretic, neuroprotective, and immunomodulatory properties (Das and Bisht, 2013). We have previously reported its ability to induce apoptosis, interfere with cell-cycle

progression and induce differentiation in leukemia cells (Fimognari et al., 2011; Ferruzzi et al., 2013). Aim of this study was to evaluate the *in vitro* anti-angiogenic potential of HI on human umbilical vein endothelial cells (HUVECs) and delineate the main molecular mechanisms involved in its anti-angiogenic activity both in normoxia and hypoxia.

Materials and methods

Materials and cell cultures

Dimethylsulfoxide (DMSO), fetal bovine serum (FBS), antibiotics (penicillin and streptomycin), trypsin-EDTA, and human recombinant VEGF were obtained from Sigma Aldrich (St. Louis, MO, USA). HUVECs were purchased from Lonza (Basel, Switzerland), cultured in EGM complete medium supplemented with SingleQuots™ (containing hydrocortisone, hEGF, FBS, VEGF, hFGF-B, R3-IGF-1, ascorbic acid, heparin and gentamycin/amphotericin-B, Lonza) and incubated at 37°C and 5% CO_2 in normoxia (21% O_2) or hypoxia (2.5% O_2). The hypoxia was guarantee by the use of the hypoxic station InVivo$_2$ 200 (Baker Ruskinn, Sanford, MA, USA). To maintain the exponential growth, cells were divided when they reached 80% of confluence in a 25 cm^2 dish. HUVECs at passage between 3 and 8 were used for the experiments.

Plant materials

HI (voucher #MAPL/20/178) was obtained from Ram Bagh (Rajasthan, India) after its authentication by Dr. MR Uniyal, Maharishi Ayurveda Product Ltd., Noida, India. The ayurvedic crude drug was collected in 2010, in particular, following the indications of Ayurvedic Pharmacopoeia of India (2004), during the balsamic period (January). The decoction was prepared according to the method previously described and agreeing with Ayurvedic Pharmacopoeia

(Fimognari et al., 2011). Briefly, 10 g of grinded roots were added to 300 mL of boiling water, and boiled until the suspension reached the volume of 75 mL. The yield of the decoction was 15%. HI decoction was filtered, lyophilized, and stored at room temperature. The experiments were performed by preparing a stock solution of 31 mg/mL. The suspension was centrifuged at 4,000 rpm to discard any insoluble material.

HPLC-MS analysis of plant decoction

The main phytomarkers of HI, namely 2-hydroxy-4-methoxybenzaldehyde, 3-hydroxy-4-methoxybenzaldehyde and 2-hydroxy-4-methoxybenzoic acid (Das and Bisht, 2013), were identified and quantified by HPLC-MS analysis. The reference compounds (all obtained from Sigma) were used as external standards to set up and calculate appropriate calibration curves. The calibration graphs were provided by the regression analysis of peak area of the analytes *versus* the related concentrations.

The analyses of three different batches of HI were performed on a Jasco PU-1585 Liquid Chromatograph (Jasco Corporation, Tokio, Japan) interfaced with a Jasco 1575 UV–vis detector (λ = 254 nm) and a LCQ-Duo Mass Spectrometer (Thermo Finnigan, San Jose, CA, USA), by a splitting flow T-valve. The mass spectrometer is equipped with heated capillary interface and electrospray ionization (ESI) source, operating with an Ion Trap (IT) analyzer. ESI system employed a 4.5 kV (positive polarity) and 5.0 kV (negative polarity) spray voltage and a heated capillary temperature of 200°C. The sheath gas and the auxiliary gas (nitrogen) flow rates were set to 0.75 and 1.2 L/min, respectively. ESI was optimized using 3-hydroxy-4-methoxybenzaldehyde and 2-hydroxy-4-methoxybenzoic acid for positive and negative polarity, respectively. The mass chromatograms were acquired in total ion current (TIC) modality from 50 to 400 m/z, and in MS/MS mode (multiple reaction monitoring) on the ESI generated most abundant ion,

corresponding to the pseudomolecular ion; $[M+H]^+$ at 153 m/z for 2-hydroxy-4-methoxybenzaldehyde and 3-hydroxy-4-methoxybenzaldehyde, and [M□H]□ at 167 m/z for 2-hydroxy-4-methoxybenzoic acid. The relative collision energy varied for the different compounds from 18 to 23%.

Chromatographic analyses were performed on a Phenomenex Gemini C18 column (5 □m, 150 mm x 2.0 mm I.D.) by gradient elution from A (0.1% formic acid in acetonitrile) - B (0.1% formic acid in water) 28:72 (v/v) for 7 min to A-B 55:35 (v/v) in 20 min, at the flow rate of 0.3 mL/min. The re-equilibrium time between runs was 5 min. The injection volume was 50 □L.

Preparation and GC-FID and GC-MS analyses of lipidic fraction

As previously reported *(Sarita Das and Satpal Singh Bisht* (2013) The Bioactive and Therapeutic Potential of *Hemidesmus indicus* R. Br. (Indian Sarsaparilla) Root *Phytother. Res.* 27(6):791-801; Jessica Fiori, Alberto Leoni, Carmela Fimognari, Eleonora Turrini, Patrizia Hrelia, Manuela Mandrone, Carmelina Iannello, Fabiana Antognoni, Ferruccio Poli & Roberto Gotti Ph.D. (2014): Determination of Phytomarkers in Pharmaceutical Preparations of Hemidesmus indicus Roots by Micellar Electrokinetic Chromatography and High-Performance Liquid Chromatography – Mass Spectrometry, Analytical Letters, DOI: 10.1080/00032719.2014.917423) in *H. indicus* root decoction can be detected not only hydrophilic compounds but also lipophilic ones.

Two g of decoction were exactly weighed into a 25 mL flask and then extracted with 20 mL of chloroform by ultrasound system maceration for 20 min. The residual decoction was centrifuged at 3000 rpm for 20min. The extraction was performed three times All supernatants were transferred into a 100 ml round bottom flask, then taken to dryness with a rotary vacuum evaporator. The procedure was repeated on three different batches. The dried extracts have been mixed with 100 μL BSTFA (1%TMCS) (Bis(trimethylsilyl)trifluoroacetamide+ trimethylchlorosilane**)** (Sigma-

Aldrich) for 45min at 80°C. Then 1 μL of solution were directly injected in GC.

Lupeol, lupeol acetate, β-sistosterol, β-amyrin acetate were identified by GC-MS and then quantified in GC-FID by external standard method. All standards were purchased from Extrasynthese (Genay, France). After derivatisation an appropriate calibration curve was calculated for each reference compound. The calibration graphs were provided by the regression analysis of peak area of the analytes *versus* the related concentrations.

GC-MS analysis was performed by a gas chromatograph (Model Varian GC-3800, Agilent Technologies Inc., Santa Clara, California, USA) equipped with a VF-5ms 5% poly- and 95% phenyl-dimethyl-siloxane bonded phase column (i.d., 0.25 mm; length, 30 m; film thickness, 0.25 μm, Agilent Technologies Inc., Santa Clara, California, USA), a mass spectrometer (Model Varian MS-4000, Agilent Technologies Inc., Santa Clara, California, USA) using electron impact (EI) and hooked to NIST library. Lupeol, lupeol acetate, β-sistosterol, β-amyrin acetate were identified by comparing their GC retention time and the MS fragmentation pattern. Operating conditions were as follows: injector temperature, 300 °C; carrier (helium) flow rate, 1 mL/min and split ratio, 1:50. Oven temperature was increased from 230 °C to 320 °C at a rate of 5 °C/min, followed by 7 min at 320 °C. The MS conditions were: ionization voltage, 70 eV; emission current, 10 mAmp; scan rate, 1 scan/s; mass range, 29–600 Da; trap temperature, 150°C, transfer line temperature, 300°C.

GC-FID was used for quantitative determination through the normalization method, without using correction factors: the relative peak areas for individual constituents were averaged on three different chromatograms of three indipendent reactions. The relative percentages were determined using a gas-chromatograph (Model GC-Trace, ThermoQuest Corporation, Atlanta, Georgia, USA) equipped with a FID detector maintained at 350°C and an autosampler (AS Triplus 3000, Thermo Electron Corporation, Waltham, Massachusetts, USA); all the others GC conditions were the same of GC-MS method.

Flow cytometry

All flow cytometric analyses were performed using the Guava easyCyte 5HT flow cytometer (Merck Millipore, Hayward, CA, USA).

Cell viability and proliferation

HUVECs were treated with HI (0.00-0.93 mg/mL) for 6 h and 24 h in normoxia and hypoxia. Viability was determined immediately after the end of treatment. Briefly, HUVECs were mixed with an adequate volume of Guava ViaCount Reagent (containing propidium iodide, Merck Millipore) and allowed to stain 5 min at room temperature before the flow cytometric analysis.

Analysis of apoptosis

The pro-apoptotic potential of HI (0.00-0.93 mg/mL) was analyzed after treatment of confluent HUVECs for 6 and 24 h in normoxia and hypoxia. Briefly, aliquots of $2x10^4$ cells were stained with 100 µL of Guava Nexin Reagent (Merck Millipore), containing Annexin V-phycoerythrin (Annexin V-PE) and 7-amino-actinomycin D (7-AAD). The samples were incubated for 20 min at room temperature in the dark and then analyzed by flow cytometry.

Endothelial cell tube formation assay

The ability of HI to influence the endothelial cell tube formation was analyzed by using the *In Vitro* Angiogenesis Assay Kit (ECM625, Merck Millipore). The assay is based on culturing cells

in an ECMatrix™, a solid gel of basement proteins prepared from the Engelbreth Holm-Swarm (EHS) mouse tumor and consisting of laminin, collagen type IV, heparan sulfate proteoglycans, entactin and nidogen. It also contains growth factors (TGF-β, FGF) and proteolytic enzymes (plasminogen, tPA, MMPs). The gel is optimized for maximal tube-formation. Thus, endothelial cells can rapidly align and form tube-like structures. Briefly, each well, of a 96-well plate, was coated with 50 µl of cold ECMatrix™ solution and the plate was kept at 37°C for 1 h to allow the solidification of the ECMatrix™. Afterwards, $1x10^4$ HUVECs were seeded in each well in a total volume of 150 µL of EGM medium and treated for 6 h in hypoxia or normoxia with various concentrations of HI (0.00–0.93 mg/mL) or VEGF 10µg/mL as positive control, alone or in association. Pictures from three randomly selected fields were taken using a Motic AE21 microscope (Campbell, CA, USA) and a VisiCam 3.0 videocamera (VWR International PBI, Milan, Italy). The capillary tube branch points formed were counted in four random view-field *per* well.

Analysis of angiogenic proteins

After treatment with HI (0.00-0.93 mg/mL) in both oxygen conditions, aliquots of $1x10^6$ HUVECs were fixed with a solution of 4% paraformaldehyde and permeabilized with ice cold 90% methanol. Afterward, cells were incubated for 30 min with anti-VEGF (1:500, Abcam, San Francisco, CA, USA) or anti-HIF-1α (1:500, Merck Millipore) antibodies, washed and incubated with the FITC-conjugated secondary antibody (1:500, Sigma). For VEGFR-2, $1x10^6$ cells were stained with 2.5 µL of anti-VEGFR-2-PE Cy-5.5 antibody (2.5:10, Biolegend, San Diego, CA, USA). Mean fluorescence intensity was quantified by flow cytometry through the analysis of 10,000 events/sample. In order to exclude non-specific bindings, the fluorescence of the isotype negative control antibody [FITC Mouse IgG1, k (FC), Biolegend] was analyzed.

RNA extraction and analysis of gene expression

After treatment for 6 h with HI (0.00-0.93 mg/ml) both in normoxia and in hypoxia, total RNA extraction was performed by miRVana^{TM} miRNA Isolation kit (Life Technologies, Carlsbad, CA, USA) according to manufacturer's instructions. Total RNA was reverse transcribed using the High Capacity cDNA reverse transcription kit (Life Technologies). RNA extraction and cDNA transcription were performed as reported above. Relative quantification of VEGF, HIF and VEGFR-2 mRNA as well as 18S and GAPDH, as internal controls, was performed by real time PCR (ABI PRISM 7900HT, Life Technologies) using Universal Master Mix and TaqMan assay (Hs00900054_m1, Hs00153153_m1, Hs00176676_m1, Hs99999901_s1, Hs99999905_m1, respectively) (Life Technologies). Each measure was performed in triplicate. Data were analyzed through $2^{-\Delta\Delta Ct}$ method.

Migration and invasion assays

Cell migration and invasion assays were performed by QCM™ 24-well Fluorimetric Cell Migration Kit (ECM509; Merck Millipore) and QCM™ 24-well Fluorimetric Cell Invasion Assay Kit (ECM554; Merck Millipore), respectively, according to the manufacturer's instructions. Both assays exploit a polycarbonate membrane with an 8 µm pore size, which in the invasion assay is coated with a thin layer of ECMatrix™ occluding the membrane pores and physically inhibits the passage of non-invasive cells. The two kits possess several common procedure steps. Briefly, HUVECs treated with HI (0.00-0.93 mg/mL) in normoxia and hypoxia were loaded in the upper compartments, while in the lower chambers EGM supplemented with 10% FBS was used as chemoattractant. The plates were incubated for 6 h for the migration and 24 h for the invasion

assay. Cells able to migrate through or invade the support were detached from the bottom using a Cell Detachment Buffer, and then fixed and stained with CYQuant GR Dye. The fluorescence of the migrated or invaded cells was evaluated by Infinity F200 Proplate reader (Tecan, Männedorf, Swiss) using 480/520 nm filter set. The migrated and invaded cell number relative variation was obtained comparing the mean fluorescence signal of HI-treated samples with untreated cells.

Statistical analysis

All experiments were repeated at least three times and results are reported as the mean ± SEM. Differences among treatments were assessed by one-way ANOVA, followed by Dunnett or Bonferroni as post-hoc test. GraphPad InStat version 5.0 (GraphPad Prism, San Diego, CA, USA) was used for all statistical analyses. $P < 0.05$ was considered significant.

Results

HI main phytomarkers

2-hydroxy-4-methoxybenzaldehyde, 3-hydroxy-4-methoxybenzaldehyde and 2-hydroxy-4-methoxybenzoic acid were indentified in HI as reference phytomarkers (Fig. 1). The amount of each phytomarker in the decoction (31 mg/mL) was quantified in: 3.06±0.2 µg/mL for 2-hydroxy-4-methoxybenzaldehyde, 20.40±0.8 µg/mL for 3-hydroxy-4-methoxybenzaldehyde, 20.02±0.7 µg/mL for 2-hydroxy-4-methoxybenzoic acid. Three different batches of HI were analyzed and no significant difference was found in the content of the three phytomarkers (data not shown).

Moreover lupeol, lupeol acetate, β-sistosterol, β-amyrin acetate were quantified in dried decoction after maceration with chloroform and results are showed in (Table 1). All these lipophilic

molecules were previously detected in the root (Das et al., 2013), but in our paper were quantified in decoction for the first time.

HI affects proliferation of HUVECs

To preliminary exclude any possible effect of HI on angiogenesis connected with the reduction of viability, the cytotoxic potential of HI on HUVECs was screened. In both normoxia and hypoxia, none of the tested concentrations showed a significant reduction in cell viability (data not shown).

In order to determine the effect of HI on HUVEC proliferation, cells were treated with different concentrations (0.00-0.93 mg/mL) for 6 h and 24 h in normoxia (Fig. 2A) and hypoxia (Fig. 2B). Treatment with HI for 6 h induced a reduction of cell proliferation by more than 30% only in normoxia and at the highest tested dose. After 24 h of treatment, a reduction of cell growth by more than 30% was induced by HI 0.62 mg/mL in normoxia, while in hypoxia a similar effect was induced by HI 0.93 mg/mL.

HI inhibits the formation of new vessels

The ability of HUVECs to migrate, attach each other, and form tube structures on ECMatrix™ is shown in Fig. 3A. HI strongly inhibited tube formation at the highest tested concentrations (0.62 and 0.93 mg/mL), in both hypoxia and normoxia (Fig. 3A). Count of the tube branch points formed after HI 0.62 mg/mL treatment showed its ability to significantly reduce the branch point number more in normoxia than in hypoxia (0.17±0.07 *vs* 0.22±0.13) compared to the untreated samples (Fig. 3B). Similar effects were recorded in cells treated with the association HI

0.62 mg/mL-VEGF, with a significant reduction of the branch point number in normoxia (0.21±0.06) and hypoxia (0.24±0.20) compared to the VEGF control (Fig. 3C). Moreover, in samples treated with HI 0.93 mg/mL in both normoxia and hypoxia, HUVECs were not able to form hollow tube-like structures. Thus, branch point could not be determined (Fig. 3B-C). Notably, HI 0.31 mg/mL appeared to stimulate angiogenesis, but the number of tube branches was not significantly increased compared to the untreated and VEGF controls in both O_2 conditions (Fig. 3B-C).

HI modulates the expression of proteins involved in the angiogenic process

The ability of HI to inhibit angiogenesis was confirmed by testing its ability to induce a post-transcriptional and post-translational modulation of proteins involved in the regulation of vessel formation process. The expression of VEGF, VEGFR-2 and HIF-1α was quantified by measuring the mean fluorescence intensity. In hypoxia and normoxia, HI induced a dose-dependent down-regulation of VEGF, which reached the highest effect at the highest tested concentration (0.81±0.02 in normoxia and 0.77±0.11 in hypoxia) (Fig. 4A). In normoxia, HI did not show any effect on the expression of VEGFR-2 and HIF-1α (Fig. 4B-C). On the other hand, in hypoxia HI down-regulated the expression of all three proteins at all tested doses. In particular, the highest effects on VEGFR-2 and HIF-1α were observed after treatment with HI 0.93 mg/mL, which induced a reduction in their expressions by 40% and 17%, respectively (Fig. 4B-C). In hypoxia, HI reduced the expression of VEGFR-2 and HIF-1α compared to the same treatments conducted at normal O_2 pressure (Fig. 4B-C).

HI inhibits VEGF, VEGFR-2 and HIF gene expression

HI modulated VEGF, VEGFR-2 and HIF gene expression. A dose-dependent down-regulation was observed, particularly marked in hypoxia (Fig. 5). The highest inhibitory effect was observed after treatment of HUVECs with HI 0.93 mg/mL, where a stronger down-regulation of HIF-1α and VEGF mRNA was recorded in hypoxia than in normoxia (0.07±0.04 *vs* 0.25±0.06 and 0.50±0.03 *vs* 1.00±0.07, respectively) (Fig. 5C). With regard to VEGFR mRNA, we observed a down-regulation both in normoxia and hypoxia (Fig. 5A).

HI inhibits cell migration and invasion

Migration plays an important role in angiogenesis and is a prerequisite for tumor-cell invasion and metastasis. We explored whether HI was able to inhibit HUVECs migration and invasion. In normoxia, the inhibition of migration and invasion was more pronounced than in hypoxia (Fig. 6A-B). Actually, HI at the highest tested concentration (0.93 mg/mL) and after 6 h of treatment led to a more pronounced reduction of the migrated cell relative variation in normoxia compared to hypoxia (0.65±0.01 *vs* 0.789±0.003, respectively) (Fig. 6A). In the same way, the invaded cell relative variation was 0.50±0.03 in normoxia *versus* 0.63±0.07 in hypoxia (Fig. 6B).

Discussion

Here, we provide first evidence that HI exerts antiangiogenic properties that could contribute to its cancer therapeutic potential. The model used covers multiple steps relevant of angiogenesis, such as endothelial cell proliferation, formation of capillary-like structures, quantification of the sprouting, endothelial cell migration and invasion. Of note, those events were analyzed also in hypoxia, which represents a tumor microenvironment strongly stimulating tumor angiogenesis.

Angiogenesis has been identified as a hallmark of tumor progression and anti-angiogenic

therapy has become a new anticancer strategy. Nowadays, numerous anti-angiogenic therapeutics are used in association with cytotoxic drugs (Cesca et al., 2013), or in maintenance treatment (Johnsson et al., 2013). Several plant products and extracts, endowed with multiple pharmacological activities, modulate many key factors involved in the complex regulation of the angiogenesis signaling pathway. Among those, fucoidan from *Undaria pinnatifida* (Liu et al., 2012), *Trifolium pretense* L. (Krenn and Paper, 2009), or *Rhizoma rhei* extracts (He et al., 2011) inhibit angiogenesis thorough the modulation of the VEGF pathway.

HI inhibited angiogenesis in normoxia and hypoxia through the regulation of key factors of the neovascularization process. Endothelial cell proliferation is strictly correlated with the angiogenic and metastatic process (Browne et al., 2006). In both O_2 conditions, HI reduced proliferation without showing any cytotoxic effect.

HI inhibited microvessel outgrowth in a dose-dependent manner, also in association with VEGF, a well-know angiogenesis inducer. The expression levels of the principal proteins involved in the angiogenesis regulation (HIF-1α, VEGF and VEGFR-2) and their mRNAs were analyzed after treatment with HI. A down-regulation of HIF-1α protein level was observed in hypoxia, while in normoxia no modulation was reported. At gene level, HI induced a dose-dependent reduction in the expression of HIF-1α, both in normoxia and hypoxia, with the highest down-regulation observed in hypoxia. Because VEGF receptors are mainly expressed on endothelial cells (Terman et al., 1991), we included the high-affinity receptor tyrosine kinase VEGFR-2 to our investigations. Between the two VEGF receptors, VEGFR-2 appears to be the major transducer of VEGF signals in endothelial cells (Jung et al., 2009). In the light of these considerations, inhibition of VEGFR-2 might represent an interesting approach for anti-angiogenic interventions. HI reduced VEGFR-2 protein expression in hypoxia and down-regulated VEGFR-2 mRNA both in hypoxia and normoxia.

Taken together, our results suggest that the inhibition of angiogenesis by HI is mediated through two distinct mechanisms according to the oxygen availability. In normoxia, the reduced

expression of VEGF seems to be the main cause of angiogenesis inhibition. On the other hand, the angiogenesis inhibition induced in hypoxia is regulated by a more complex mechanism involving firstly HIF-1α inhibition, followed by VEGF and VEGFR-2 down-regulation.

Blood vessel formation is the result of multiple molecular events, where VEGF constitutes one of the central factors. It acts as an endothelial mitogen and induces endothelial cell survival, migration, differentiation, and self-assembly (Affara and Robertson, 2004). VEGF mRNA expression is regulated by HIF-1α and NF-κB (Josko and Mazurek, 2004). HIF-1 is an oxygen-dependent transcriptional activator: in normoxia, HIF-1α is degraded by the proteasome after post-transcriptional modification; under hypoxia, HIF-1α is stable, translocates to the nucleus and favours transcription of >60 target genes, including VEGF (Semenza, 2003). HI strongly reduced the mRNA level of HIF-1 both in normoxia and hypoxia. However, it evokes a differential regulation at protein level: a down-regulation was evident only in hypoxia. A lack of correlation between mRNA and protein abundance is common. Indeed, proteins have very different half-lives due to the result of varied protein synthesis and degradation, and varied post-transcriptional mechanisms involved in turning mRNA into protein. Downregulation of mRNA concurrent with upregulation of protein expression may occur when a protein half-life is increased due to stabilization components involved gwith the protein's normal turnover or the protein may be stabilized through protein-protein interactions. Further esperiments could assess the modulation by HI of microRNAs that moderate the HIF-1α transcriptional program and of the proteasome-mediate degradation of HIF-1 normoxia.

Of note, previous studies reported that NF-κB is a direct modulator of HIF-1α expression (van Uden et al., 2008) and regulates endothelial cell integrity and vascular homeostasis *in vivo*, also through the modulation of VEGF mRNA expression (Josko and Mazurek, 2004). For example, zerumbone derived from a subtropical ginger, *Zingiber zerumbet* Smith, inhibits tumor angiogenesis

via NF-κB in gastric cancer (Tsuboi et al., 2014). Additionally, suppression of NF-κB activity abrogated the NF-κB activation and the pro-angiogenic activities of glioma cells (Jiang et al., 2013). Very recently, it was reported that HI prevented active NF-κB from binding to its nuclear DNA (Guerrini et al., 2014). Consequently, NF-kB-regulated mechanisms, including HIF-1 and VEGF expression, involved in proangiogenic signaling under hypoxia might be sensitive to HI treatment.

Neovascularization influences the dissemination of cancer cells throughout the entire body, eventually leading to metastasis formation. The vascularization level of a solid tumor is an excellent indicator of its metastatic potential (Nishida et al., 2006). In this context, HI significantly suppressed invasion and migration of endothelial cells. These activities were not due to the antiproliferative influence of HI, because they were observed under experimental conditions (0.31 mg/mL in hypoxia and normoxia and 0.62 mg/mL in hypoxia) where cell proliferation was not impeded. Low oxygen conditions accelerate cell invasion (Miyoshi et al., 2006), justifying the less pronounced inhibition of invasion resulted from HI treatments in hypoxia than in normoxia.

On the bases of its multiple anticancer mechanisms, HI can represent an interesting botanical drug. The chemical constituents of a botanical drug are not always well defined. In many cases, the active constituent is not identified nor is its biological activity characterized. Accordingly, there is a concern about the therapeutic consistency of marketed batches of a botanical drug (Fimognari et al., 2012). As far as the therapeutic consistency of HI is concerned, our HPLC phytochemical analysis demonstrated the presence of 2-hydroxy-4-methoxybenzaldehyde, 3-hydroxy-4-methoxybenzaldehyde, 2-hydroxy-4-methoxybenzoic acid and for the first time lupeol acetate, together to minor compounds as lupeol, beta-sitosterol, beta-amyrin acetate which can be used as fingerprint. Interestingly, vanillin (4-hydroxy-3-methoxybenzaldehyde, a structural analogue lupeol have been shown to possess antiangiogenic activity (Jung et al, 2010; Lirdprapamongkol et al, 2009; Vijay Avin et al., 2014). The phytochemical analysis performed on

three batches of HI demonstrated that the levels of the seven phytomarkers were not statistically different among batches. Of note, the three batches were not statistically different in terms of biological activities.

The findings of this study suggest that the antiangiogenic activity of HI is based on multiple interactions with critical steps in the angiogenic cascade. VEGF expression stimulated by HIF-1α as well as endothelial cell migration and differentiation represent important targets of HI action and might contribute to its cancer therapeutic efficacy that is presently emerging.

Conflict of interest

The authors declare no conflict of interests.

Acknowledgments

This work was supported by Fondazione Cassa di Risparmio di Imola and Italian Ministry of University and Research through the PRIN 2009 (project number 2009LR9YLF to G.S.). We are also grateful to Prof. Ferruccio Poli, Department of Pharmacy and BioTechnology, *Alma Mater Studiorum*-University of Bologna, for providing us with the decoction of *Hemidesmus indicus*.

References

Affara, N.I., Robertson, F.M., 2004.Vascular endothelial growth factoras as urvival factor in tumor-associated angiogenesis. In Vivo 18,525–542.

Ayurvedic Pharmacopoeia of India, part 1, vol. IV, Government of India, Ministry of Health and Family Welfare, Department of Ayush, 2004.

Browne, C.D., Hindmarsh, E.J., Smith, J.W., 2006. Inhibition of endothelial cell proliferation and angiogenesis by orlistat, a fatty acid synthase inhibitor. The FASEB Journal 20, 2027–2035.

Cesca, M., Bizzaro, F., Zucchetti, M., Giavazzi, R., 2013. Tumor delivery of chemotherapy combined with inhibitors of angiogenesis and vascular targeting agents. Frontiers in Oncology 3, 259.

Costa-Lotufo, L.V., Khan, M.T., Ather, A., Wilke, D.V., Jimenez, P.C., Pessoa, C., de Moraes, M.E., de Moraes, M.O., 2005. Studies of the anticancer potential of plants used in Bangladeshi folk medicine. Journal of Ethnopharmacology 99, 21–30.

Das, S., Bisht, S.S., 2013. The bioactive and therapeutic potential of Hemidesmus indicus R. Br. (Indian Sarsaparilla) root. Phytotherapy Research 27, 791–801.

Elice, F., Rodeghiero, F.,2012. Side effects of anti-angiogenic drugs. Thrombosis Research 129 (Suppl.1), S50–S53.

Ferruzzi, L., Turrini, E., Burattini, S., Falcieri, E., Poli, F., Mandrone, M., Sacchetti, G., Tacchini, M., Guerrini, A., Gotti, R., Hrelia, P., Cantelli-Forti, G., Fimognari, C., 2013. Hemidesmus indicus induces apoptosis as well as differentiation in a human promyelocytic leukemic cell line. Journal of Ethnopharmacology 147, 84–91.

Fimognari, C., Ferruzzi, L., Turrini, E., Carulli, G., Lenzi, M., Hrelia, P., Cantelli-Forti, G., 2012. Metabolic and toxicological considerations of botanicals in anticancer therapy. Expert Opinion in Drug Metabolism and Toxicology 8, 819–832.

Fimognari,C., Lenzi, M., Ferruzzi, L., Turrini, E., Scartezzini, P., Poli, F., Gotti, R., Guerrini, A., Carulli, G., Ottaviano, V., Cantelli-Forti, G., Hrelia, P., 2011. Mitochondrial pathway mediates the antileukemic effects of Hemidesmus indicus, a promising botanical drug. PLoSOne 6, e21544.

Fiori, J., Leoni, A., Fimognari, C., Turrini, E., Hrelia, P., Mandrone, M., Iannello, C., Antognoni, F., Poli, F., Gotti, R., 2014. Determination of phytomarkers in pharmaceutical preparations of Hemidesmus indicus roots by micellar electrokinetic chromatography and high-performance liquid chromatography–mass spectrometry. Analytical Letters , http://dx.doi.org/10.1080/00032719.2014.917423.

Foekens, J.A., Peters, H.A., Grebenchtchikov, N., Look, M.P., Meijer-vanGelder, M.E., Geurts-Moespot, A., vanderKwast, T.H., Sweep, C.G., Klijn, J.G., 2001. High tumor levels of vascular endothelial growth factor predict poor response to systemic therapy in advanced breast cancer. Cancer Research 61, 5407–5414.

Guerrini, A., Mancini, I., Maietti, S., Rossi, D., Poli, F., Sacchetti, G., Gambari, R., Borgatti, M., 2014. Expression of pro-inflammatory interleukin-8 is reduced by Ayurvedic decoctions. Phytotherapy Research , http://dx.doi.org/10.1002/ptr.5109.

He, Z.H., Zhou, R., He, M.F., Lau, C.B., Yue, G.G., Ge, W., But, P.P., 2011. Antiangiogenic effect and mechanism of rhein from Rhizoma Rhei. Phytomedicine 18, 470–478.

Jain, R.K., 2005. Normalization of tumor vasculature: an emerging concept in antiangiogenic therapy. Science 307, 58–62.

Jiang, L., Song, L., Wu, J., Yang, Y., Zhu, X., Hu, B., Cheng, S.Y., Li, M., 2013. Bmi-1 promotes glioma angiogenesis by activating NF-kappaB signaling. PLoSOne 8, e55527.

Johnsson, A., Hagman, H., Frodin, J.E., Berglund, A., Keldsen, N., Fernebro, E., Sundberg, J., DePont, C.R., GarmSpindler, K.L., Bergstrom, D., Jakobsen, A., 2013. A randomized phaseIII trial on maintenance treatment with bevacizumab alone or in combination with erlotinib after chemotherapy and bevacizumab in metastatic colorectal cancer: the Nordic ACT Trial. Annals of Oncology 24, 2335–2341.

Josko, J., Mazurek, M., 2004. Transcription factors having impact on vascular endothelial growth factor (VEGF) gene expression in angiogenesis. Medical Science Monitor 10, RA89–RA98.

Jung, M.H., Lee, S.H., Ahn, E.M., Lee, Y.M., 2009. Decursin and decursinolangelate inhibit VEGF-induced angiogenesis via suppression of the VEGFR-2-signaling pathway. Carcinogenesis 30, 655–661.

Jung, H.J., Song, Y.S., Kim, K., Lim, C.J., Park, E.H., 2010. Assessment of the antiangiogenic, anti-inflammatory and antinociceptive properties of ethylvanillin. Archives of Pharmacal Research 33, 309–316.

Krenn, L., Paper, D.H., 2009. Inhibition of angiogenesis and inflammation byan extract of redclover (Trifolium pratense L.). Phytomedicine 16, 1083–1088.

Kumar, R., Harris-Hooker, S., Kumar, R., Sanford, G., 2011. Co-culture of retinal and endothelial cells results in the modulation of genes critical to retinal neovascularization. Vascular Cell 3, 27.

Kuschel, A., Simon, P., Tug, S., 2012. Functional regulation of HIF-1 alpha under normoxia is there more than post-translational regulation? Journal of Cellular Physiology 227, 514–524.

Lirdprapamongkol, K., Kramb, J.P., Suthiphongchai, T., Surarit, R., Srisomsap, C., Dannhardt, G., Svasti, J., 2009. Vanillin suppresses metastatic potential of human cancer cells through PI3K inhibition and decreases angiogenesis in vivo. Journal of Agricultural and Food Chemistry 57, 3055–3063.

Liu, F., Wang, J., Chang, A.K., Liu, B., Yang, L., Li, Q., Wang, P., Zou, X., 2012. Fucoidan extract derived from Undaria pinnatifida inhibits angiogenesis by human umbilical vein endothelial cells. Phytomedicine 19, 797–803.

Marriott, J.F., Wilson, K.A., Langley, C.A., Belcher, D., 2006. Pharmaceutical Compounding and Dispensing. Pharmaceutical Press, London.

Mary, N.K., Achuthan, C.R., Babu, B.H., Padikkala, J., 2003. In vitro antioxidant and antithrombotic activity of Hemidesmus indicus (L) R.Br. Journal of Ethnopharmacology 87, 187–191.

Miyoshi, A., Kitajima, Y., Ide, T., Ohtaka, K., Nagasawa, H., Uto, Y., Hori, H., Miyazaki, K., 2006. Hypoxia accelerates cancer invasion of hepatoma cells by upregulating MMP expression in an HIF-1 alpha-independent manner. International Journal of Oncology 29, 1533–1539.

Nishida, N., Yano, H., Nishida, T., Kamura, T., Kojiro, M., 2006. Angiogenesis in cancer. Vascular Health and Risk Management 2, 213–219.

Parangi, S., O'Reilly, M., Christofori, G., Holmgren, L., Grosfeld, J., Folkman, J., Hanahan, D., 1996. Antiangiogenic therapy of transgenic mice impairs denovo tumor growth. Proceedings of the National Academy of Sciences of the United States of America 93, 2002–2007.

Reynolds, A.R., 2010. Potential relevance of bell-shaped and u-shaped dose– responses for the therapeutic targeting of angiogensis in cancer. Dose Response 8, 253–284.

Samarakoon, S.R., Thabrew, I., Galhena, P.B., Tennekoon, K.H., 2012. Modulation of apoptosis in human hepatocellular carcinoma (HepG2 cells) by a standardized herbal decoction of Nigella sativa seeds, Hemidesmus indicus roots and Smilax glabra rhizomes with anti-hepatocarcinogenic effects. BMC Complementary and Alternative Medicine 12, 25.

Semenza, G.L., 2003. Targeting HIF-1 for cancer therapy. Nature Reviews Cancer 3, 721–732.

Suffness, M., Pezzuto, J.M., 1990. Assays related to cancer drug discovery. In: Hostettmann, K. (Ed.), Methods Plant

Biochemistry: Assays for Bioactivity. Academic Press, London, pp.71–133.

Terman, B.I., Carrion, M.E., Kovacs, E., Rasmussen, B.A., Eddy, R.L., Shows, T.B., 1991. Identification of a new endothelial cell growth factor receptor tyrosine kinase. Oncogene 6, 1677–1683.

Thabrew, M.I., Mitry, R.R., Morsy, M.A., Hughes, R.D., 2005. Cytotoxic effects of a decoction of Nigella sativa, Hemidesmus indicus and Smilax glabra on human hepatoma HepG2 cells. Life Sciences 77, 1319–1330.

Tsuboi, K., Matsuo, Y., Shamoto, T., Shibata, T., Koide, S., Morimoto, M., Guha, S., Sung, B., Aggarwal, B.B., Takahashi, H., Takeyama, H., 2014. Zerum bone inhibits tumor angiogenesis via NF-kappaB in gastric cancer. Oncology Reports 31, 57–64.

Van Uden, P., Kenneth, N.S., Rocha, S., 2008. Regulation of hypoxia-inducible factor 1alpha by NF-kappaB. The Biochemical Journal 412, 477–484.

Zarei, M., Javarappa, K.K., 2012. Anticarcinogenic and cytotoxic potential of Hemidesmus indicus root extract against Ehrlich Ascites tumor. Der Pharmacia Lettre 4, 906–910.

Table 1. Quantification of lipophilic compounds

Compound	μg/mL
Lupeol	1.47±0.06
Lupeol acetate	24.58±1.32
β-sitosterol	1.66±0.23
β-amyrin acetate	2.95±0.18

Figure legends

Fig. 1. LC-MS SIM (single ion monitoring) chromatograms of the decoction. Black line: detection in positive polarity of 3-hydroxy-4-methoxybenzaldehyde (1) and 2-hydroxy-4-methoxybenzaldehyde (2). Dashed line: detection in negative polarity of 2-hydroxy-4-methoxybenzoic acid (3).

Fig. 2. HUVEC proliferation after treatment with HI (0.00-0.93 mg/mL) for 6 h and 24 h in normoxic (A) and hypoxic (B) conditions.

Fig. 3. Microscopic photographs of HUVEC tube formation on ECMatrix™ after HI treatment for 6 h in normoxia and hypoxia (A). (a, a1) untreated cells; (b, b1) VEGF 10 µg/mL; (c, c1) *Hemidesmus* 0.31 mg/mL; (d, d1) 0.62 mg/mL; (e, e1) 0.93 mg/mL. Branch point relative variation after HUVEC treatment for 6 h in normoxia and hypoxia with HI or VEGF (B) and their association (C).

Fig. 4. Relative protein expression (RE) of VEGF (A), VEGFR-2 (B) and HIF-1α (C) in HUVECs after treatment with HI for 6 h.

Fig. 5. Relative mRNA expression of VEGF (A), VEGFR-2 (B) and HIF (C) after treatment of HUVECs with HI for 6 h.

Fig. 6. Relative variation of HUVEC migrated (A) and invaded (B) cell number following HI treatment for 6 or 24 h in normoxic and hypoxic conditions.

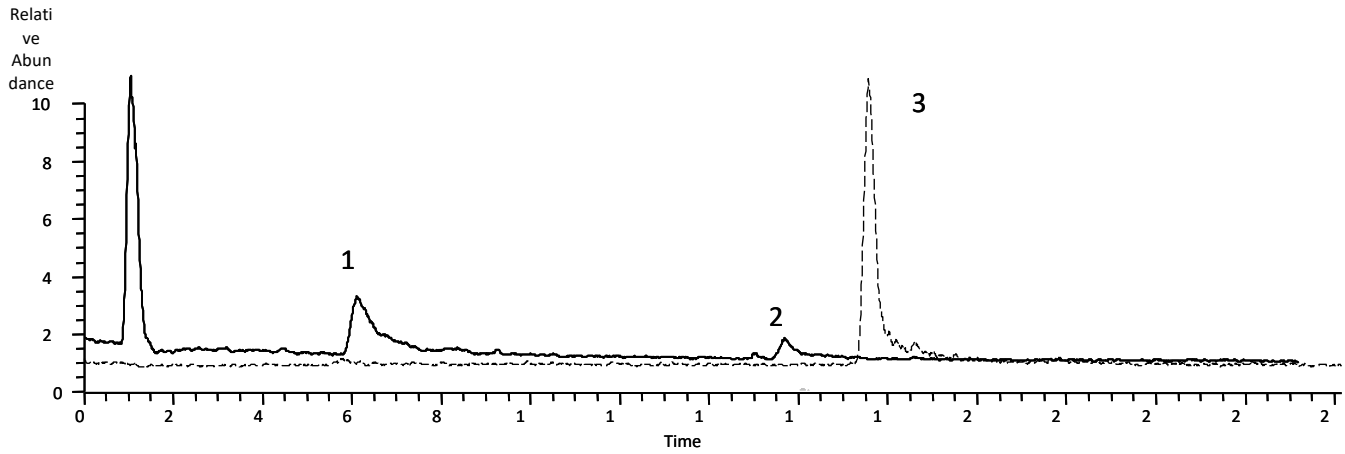

Fig. 1

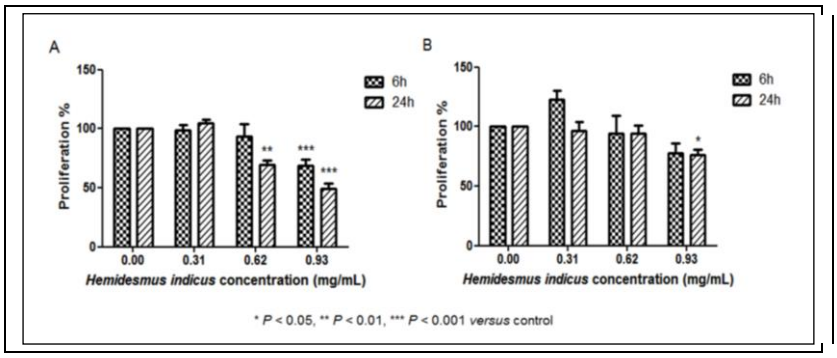
A
B
6h
24h
Proliferation %
150
100
50
0
0.00
0.31
0.62
0.93
**
***
***
*
Hemidesmus indicus concentration (mg/mL)
* P < 0.05, ** P < 0.01, *** P < 0.001 versus control

Fig. 2

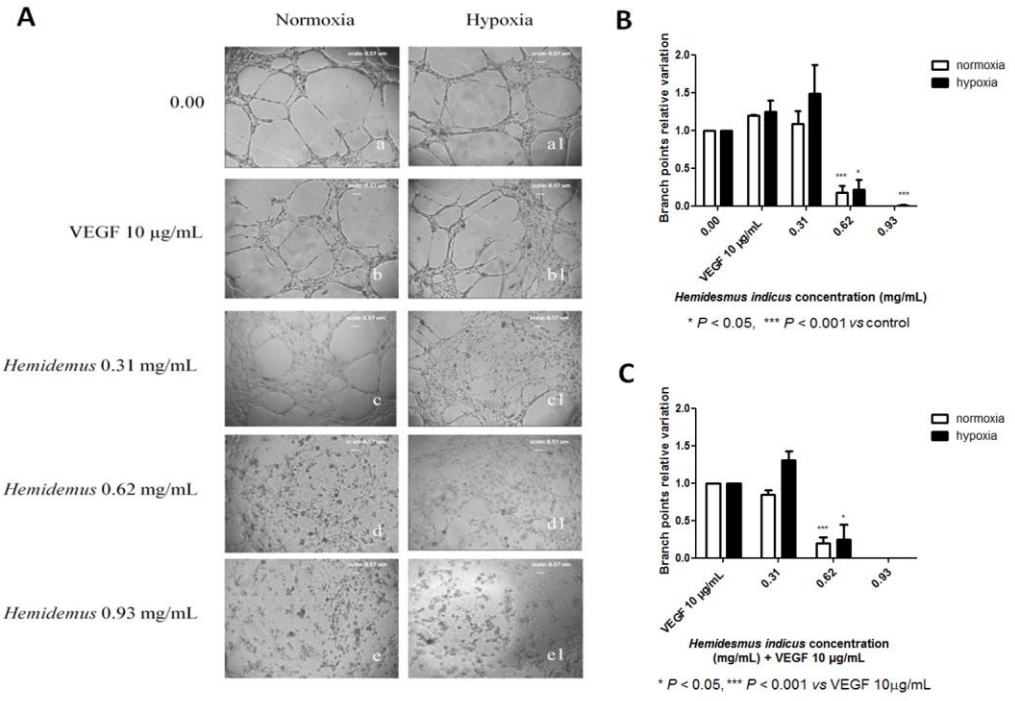
A
Normoxia
Hypoxia
0.00
VEGF 10 µg/mL
Hemidemus 0.31 mg/mL
Hemidemus 0.62 mg/mL
Hemidemus 0.93 mg/mL
a
a1
b
b1
c
c1
d
d1
e
e1
B
Branch points relative variation
normoxia
hypoxia
0.00
VEGF 10 µg/mL
0.31
0.62
0.93
Hemidesmus indicus concentration (mg/mL)
* P < 0.05, *** P < 0.001 vs control
C
Branch points relative variation
normoxia
hypoxia
VEGF 10 µg/mL
0.31
0.62
0.93
Hemidesmus indicus concentration (mg/mL) + VEGF 10 µg/mL
* P < 0.05, *** P < 0.001 vs VEGF 10µg/mL

Fig. 3

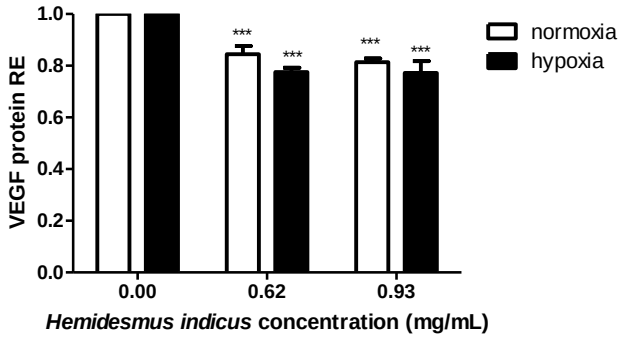

* *Hemidesmus indicus vs* control

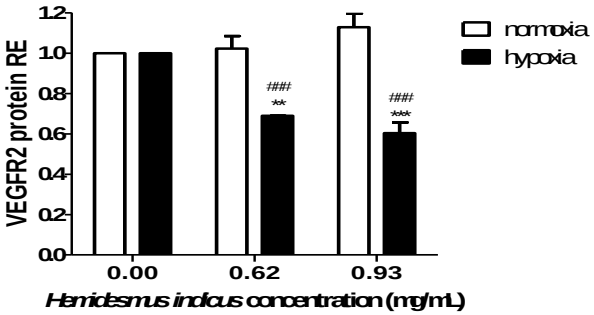

* *Hemidesmus indicus vs* control
# hypoxia *vs* normoxia

C

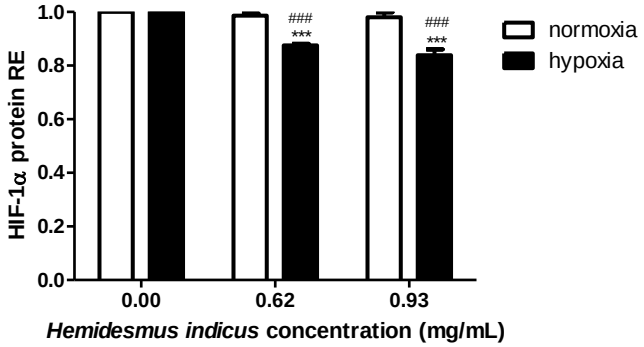

* *Hemidesmus indicus vs* control
# hypoxia *vs* normoxia
**P < 0.01, *** P < 0.001

Fig. 4

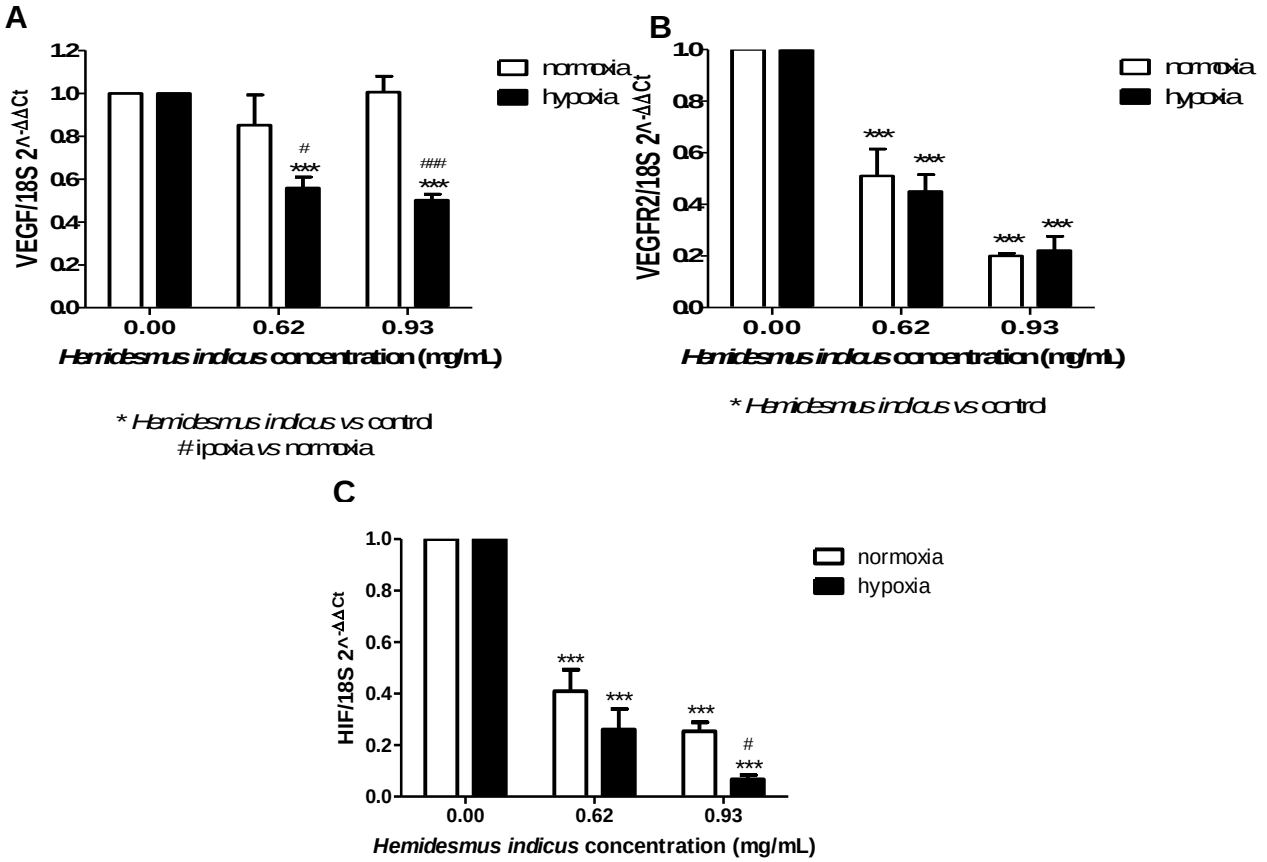
A
VEGF/18S 2^-ΔΔCt
normoxia
hypoxia
0.00
0.62
0.93
Hemidesmus indicus concentration (mg/mL)
* Hemidesmus indicus vs control
# ipoxia vs normoxia
B
VEGFR2/18S 2^-ΔΔCt
normoxia
hypoxia
0.00
0.62
0.93
Hemidesmus indicus concentration (mg/mL)
* Hemidesmus indicus vs control
C
HIF/18S 2^-ΔΔCt
normoxia
hypoxia
0.00
0.62
0.93
Hemidesmus indicus concentration (mg/mL)
* Hemidesmus indicus vs control
# ipoxia vs normoxia
*** P < 0.001
# P< 0.05, ### P < 0.001

Fig. 5

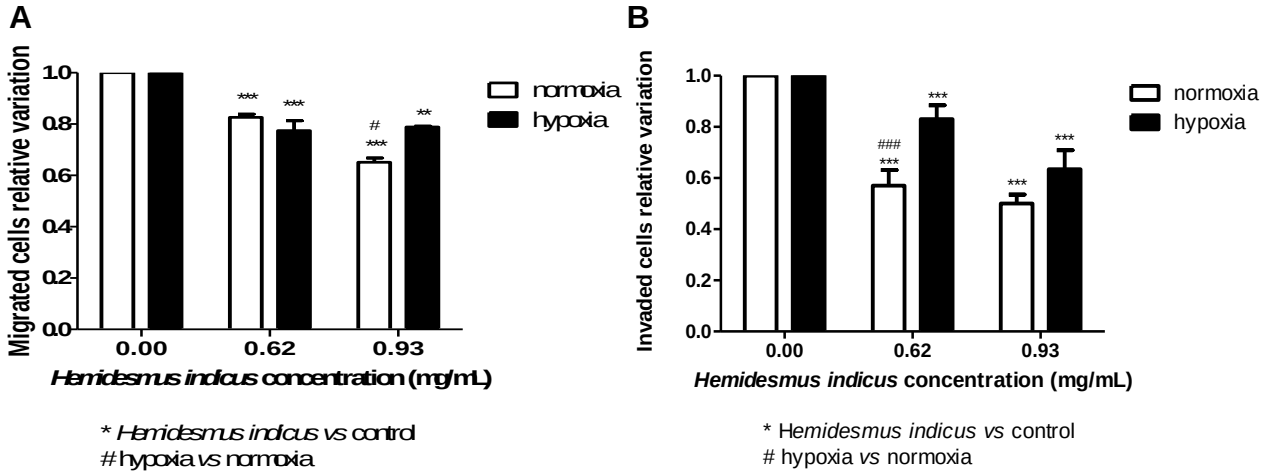

**P < 0.01, *** P < 0.001

$^{\#}$P < 0.05, $^{\#\#\#}$P < 0.001

Fig. 6

Fig. 6